International Journal of Innovative
Computing, Information and Control
Volume 11, Number 4, August 2015

 ISSN 1349-4198
pp. 1441–1456

GENERALIZED ORTHOGONAL MATCHING PURSUIT FOR DISTRIBUTED COMPRESSED SENSING

Yong Xu[1,2,3], Jing Xing[1,2,3], Yujie Zhang[1] and Hongwei Li[1,3,*]

[1]School of Mathematics and Physics
[3]Hubei Subsurface Multi-Scale Imaging Key Laboratory
China University of Geosciences
No. 388, Lumo Road, Wuhan 430074, P. R. China
xuyong654321@126.com; *Corresponding author: hwli@cug.edu.cn

[2]Institute of Statistics
Hubei University of Economics
No. 8, Yangqiaohu Ave., Jiangxia Dist., Wuhan 430205, P. R. China

Received November 2014; revised April 2015

Abstract. *In this paper, generalized orthogonal matching pursuit for distributed compressed sensing (DCS-GOMP) is proposed. As its name, the algorithm is based on orthogonal matching pursuit (OMP), but not need sparsity as prior knowledge and multiple indices are identified at each iteration for recovery. These make it a potential candidate for many practical applications, where the numbers of non-zero (significant) coefficients of signals are not available. Numerical experiments are conducted to demonstrate the validity and high performance of the proposed algorithm, compared with other existing DCS algorithms.*

Keywords: Distributed compressed sensing, Orthogonal matching pursuit, Sparsity, Correlation

1. **Introduction.** Compressed sensing (CS) [1], a paradigm to acquire sparse signals at a rate significantly below Nyquist rate, has attracted increasing interests in recent years. The major principle of CS is that sparse or compressible signals with a few significant samples can be recovered using a small number of linearly transformed measurements [2]. Assume that $\mathbf{x}$ is a signal of N-dimension, it is called K-sparse if $\mathbf{x}$ can be well represented by K ($\ll N$) coefficients under linear transformations. In CS theory, signal $\mathbf{x}$ can be reconstructed through the linear measurement system as follows:

$$\mathbf{y} = \mathbf{\Phi x} \tag{1}$$

where $\mathbf{y} \in \mathbb{R}^{M\times 1}$ is the M-dimensional measurement ($M < N$), and $\mathbf{\Phi}$ is an $M \times N$ matrix called measurement matrix. The goal of CS is to reconstruct $\mathbf{x}$ via $\mathbf{y}$. The CS framework is interesting since it indicates that $\mathbf{x}$ can be precisely recovered from only $M = O(K \log N)$ measurements, implying the potential of significant cost reduction in digital data acquisition [3]. Meanwhile, for recovering $\mathbf{x}$ perfectly, it requires the measurement matrix with low coherence [1-3]. Gaussian matrices have been proved to satisfy the condition of coherence.

A straightforward approach for recovering $\mathbf{x}$ is to translate this problem into l_0-norm minimization problem as follows:

$$\min_{\mathbf{x}} \|\mathbf{x}\|_0 \quad \text{s.t.} \quad \mathbf{\Phi x} = \mathbf{y} \tag{2}$$

Unfortunately, solving l_0-norm minimization problem is NP-hard since it contains an exhaustive search over all possible solutions, which cannot be applied for practical applications [4,5]. Hence, much research has been conducted to investigate faster recovery algorithms with moderate complexity. Donoho and Candes et al. proposed that a much easier l_1-norm optimization, based on linear programming (LP) techniques, is equivalent to the l_0-norm optimization, i.e.,

$$\min_{\mathbf{x}} \|\mathbf{x}\|_0 \quad \text{s.t.} \quad \mathbf{\Phi x} = \mathbf{y} \Leftrightarrow \quad \min_{\mathbf{x}} \|\mathbf{x}\|_1 \quad \text{s.t.} \quad \mathbf{\Phi x} = \mathbf{y} \tag{3}$$

if $\mathbf{\Phi}$ satisfies the so-called restricted isometry property (RIP) with a constant parameter [1,4-6]. Although the l_1-norm optimization technique can provide nearly optimal solution [4,5], its complexity is still a thorny problem especially for large scale applications; for instance, the complexity of LP algorithms based on interior point methods is $O(M^2N^{3/2})$ [7].

Due to the low complexity, several recovery algorithms based on iterative greedy pursuit have been researched widely in recent years, for instance, orthogonal matching pursuit (OMP) [8], improved backward optimized orthogonal matching pursuit algorithm (IBOOMP) [9], regularized OMP (ROMP) [10], compressive sampling matching pursuit (CoSaMP) [11], subspace pursuit (SP) [12] and sparsity adaptive matching pursuit (SAMP) [13].

In the past few years, researchers realize that the CS theory which is mainly designed to exploit intra-signal structures at a single sensor is not sufficient for practical applications, such as wireless sensor network (WSN). Hence, distributed compressed sensing (DCS), a new distributed coding algorithm for multi-signal ensembles that exploit both intra- and inter-signal correlation structures was proposed [14]. The DCS theory depends on the concept of joint sparsity of a signal ensemble. In a typical DCS scenario, several sensors measure signals which are each individually sparse and also correlated from sensor to sensor. Each sensor independently encodes its signal and then transmits just a number of obtained coefficients to a collection point. Under some right conditions, all of the signals can be jointly recovered by decoding at the collection point. Some researches are conducted to interpret joint sparsity for DCS. In [15] two different joint sparse models (JSM) which can be applied in different scenarios are defined to demonstrate various types of connections between these sparse signals.

Enlightened by algorithms for CS, some DCS algorithms were proposed. For instance, based on l_1-minimization technique, linear program is used to jointly recover sparse signals [16]. Additionally, some iterative greedy pursuit algorithms are developed to recover signals jointly. Simultaneous orthogonal matching pursuit (SOMP) [17] was proposed for the multi-signal joint sensing and recovery. Five greedy algorithms for DCS were proposed in [18], including simultaneous iterative hard thresholding (SIHT), simultaneous normalized IHT (SNIHT), simultaneous hard thresholding pursuit (SHTP), simultaneous normalized HTP (SNHTP), simultaneous CoSaMP (SCoSaMP). Inspired by SP algorithm, Sundman et al. develop it for DCS cases to jointly recover sparse signals [19], which is termed as Joint-SP. Unfortunately, [18,19] need sparsity as the prior information, which is not realistic in practical applications. On the other hand, the methods proposed in [14-17] cannot deal with the DCS problem based on the model in [20], which can be seen as a generalization over previously typical JSMs. As an improvement, SAMP for DCS (referred as DCS-SAMP) was proposed [20]. It has provable recovery accuracy as that of LP optimization technique, and demonstrates low complexity comparable to that of OMP methods.

In this paper a new iterative greedy algorithm is proposed to solve the DCS problem. Enlightened by the generalized orthogonal matching pursuit (GOMP) [21], DCS-GOMP

is conducted to reconstruct several input signals jointly without any prior information of sparsity. Additionally, multiple indices are identified at each iteration of DCS-GOMP for recovery. Following the same model in [20], common and individual support-sets are used in this paper to characterize jointly sparse signals. The JSM we use is also called mixed support-set model. For highlighting the advantages of DCS-GOMP, it is compared with DCS-SAMP, Joint-OMP [19] and Joint-SP [19] through several numerical simulations, in terms of the requirement of measurements and the robustness against sparsity. In order to test the validity for practical application, a DCS problem of speech signals is solved by DCS-GOMP and DCS-SAMP, respectively. And also, recovery of image is performed by the proposed algorithm. The final results sufficiently demonstrate the application potential of our algorithm.

The remainder of this paper is organized as follows. In Section 2, DCS and three different joint sparse models (JSMs) are introduced to exhibit different types of connections between the sparse signals. Section 3 discusses the proposed algorithm in detail and provides some theoretical analysis of DCS-GOMP guaranteeing perfect recovery. Simulation results which evaluate the performance of the proposed algorithm numerically are shown in Section 4. Conclusions are stated in the end of this paper.

2. **Distributed Compressed Sensing and Mixed Support-Set Model.**

2.1. **Distributed compressed sensing.**

The same DCS model of [20], which exploits both intra- and inter-signal correlation structures, is considered here. That is

$$\mathbf{y}_j = \mathbf{\Phi}\mathbf{x}_j, \quad (j = 1, 2, \ldots, L) \tag{4}$$

where each signal $\mathbf{x}_j \in \mathbb{R}^{N\times L}$. For a signal sparse in certain transformed domain, there exists a determined sparse basis $\mathbf{\Psi}$ by which $\mathbf{x}_j$ can be sparsely represented by no more than K ($\ll N$) coefficients. In case of $\mathbf{\Psi} = \mathbf{I}$, $\mathbf{x}_j$ is termed as K-sparse signal in time domain. The measurements $\mathbf{y}_j$ are obtained by using the measurement matrix $\mathbf{\Phi} \in \mathbb{R}^{M\times N}$ on $\mathbf{x}_j$ through M linear combinations. Equation (4) can also be interpreted as matrix form:

$$\mathbf{Y} = \mathbf{\Phi}\mathbf{X} \tag{5}$$

where $\mathbf{X} = (\mathbf{x}_1, \mathbf{x}_2, \ldots, \mathbf{x}_L) \in \mathbb{R}^{N\times L}$ represents the ensemble of K-sparse signals and $\mathbf{Y} = (\mathbf{y}_1, \mathbf{y}_2, \ldots, \mathbf{y}_L) \in \mathbb{R}^{M\times L}$ is the set of measurements. The goal of DCS is to simultaneously reconstruct $\mathbf{X}$ from $\mathbf{Y}$.

2.2. **Mixed support-set model.**

Three existing joint sparsity models (JSMs) that exploit the interrelation between the sparse signals in Equation (4) are demonstrated below. They are applied in different cases.

2.2.1. *JSM-1: Common sparse supports model.* In this model all signals are generated from the same sparse set of basis vectors while with various coefficients [17]:

$$\mathbf{x}_j = \mathbf{\Psi}\boldsymbol{\beta}_j, \quad (j = 1, 2, \ldots, L) \tag{6}$$

where $\boldsymbol{\beta}_j$ is supported only on the same $\Xi \subset \{1, 2, \ldots, N\}$ with $|\Xi| = K$ and K is the sparsity of $\mathbf{x}_j$. That means all signals are K-sparse with same indices but different coefficients.

2.2.2. *JSM-2: Sparse common component + innovations.* In this model, all signals share a common sparse component while each individual signal owns a sparse innovation component [17], i.e.,

$$\mathbf{x}_j = \mathbf{z} + \mathbf{z}_j, \quad (j = 1, 2, \ldots, L) \tag{7}$$

where $\mathbf{z} = \boldsymbol{\Psi}\boldsymbol{\beta}_z$, $\|\boldsymbol{\beta}_z\|_0 = K_z$ and $\mathbf{z}_j = \boldsymbol{\Psi}\boldsymbol{\beta}_j$, $\|\boldsymbol{\beta}_j\|_0 = K_j$. The l_0 norm $\|\boldsymbol{\beta}\|_0$ only counts the number of nonzero entries in vector $\boldsymbol{\beta}$. Obviously, the K_z-sparse signal $\mathbf{z}$ is common to all of the $\mathbf{x}_j$ $(j = 1, 2, \ldots, L)$. The signals $\mathbf{z}_j$ are the unique components of the $\mathbf{x}_j$ with sparsity K_j.

2.2.3. *JSM-3: Sparse common support + sparse independent innovation (mixed support-set).* This model extends JSM-2 so that there is no restriction on the associated signal values. That is, the common component is common only in the support set while nonzero coefficients of the innovation parts and common parts are various among the signals [20]. JSM-3 can be interpreted as

$$\mathbf{x}_j = \boldsymbol{c}_j + \mathbf{z}_j = \boldsymbol{\Psi}(\boldsymbol{\beta}_j + \boldsymbol{\sigma}_j), \quad (j = 1, 2, \ldots, L) \tag{8}$$

The vector $\boldsymbol{\beta}_j$ is, common among all signals, supported only on the same $\Xi \subset \{1, 2, \ldots, N\}$ with $|\Xi| = K_z$, where K_z is the sparsity of $\boldsymbol{\beta}_j$. $\boldsymbol{\sigma}_j$ is the innovation part coefficients vector with the nonzero support cardinality K_j.

One can find that Equation (8) could be seen as a generalization over Equation (6) and Equation (7). Assume each $\mathbf{x}_j$ is K-sparsity, if the interrelation among them is ignored, it roughly requires $c \times K \times L$ measurements to fully represent all of the signals and L independent reconstruction procedures. In contrast, applying the mixed support-set model, the DCS method requires only $c \cdot \left(K_c + \sum_{j=1}^{L} K_j\right)$ measurements and only one reconstruction procedure to recover the sparse signals simultaneously [20]. In this paper, DCS-GOMP is proposed for JSM-3.

3. **Generalized Distributed Orthogonal Matching Pursuit.** Some notations used in this paper are summarized below.

$\mathbf{A}^+$: the pseudo-inverse of matrix $\mathbf{A}$.

$\mathbf{A}_I$: a submatrix of $\mathbf{A}$ which is composed of the columns of $\mathbf{A}$ with indices $i \in I$.

$\mathbf{x}(I)$: a vector composed of the entries of vector $\mathbf{x}$ with indices $i \in I$.

$\mathbf{res}^k$: the residue in the k-th iteration.

$\|\mathbf{A}\|_{row-\infty}$: taking ∞-norm of matrix $\mathbf{A}$ row by row.

$\mathrm{Arg\,max}(\mathbf{x}, \mathrm{d})$: select indices corresponding to d largest elements in vector $\mathbf{x}$.

3.1. **Algorithm description.** The whole procedure of DCS-GOMP is described as follows.

Input: measurement matrix $\boldsymbol{\Phi}$, measurement $\mathbf{Y}$, the number of signals L, number of indices selected at each iteration p.

Initialization: $\hat{\mathbf{x}}_j = \mathbf{0}$ $(j = 1, 2, \ldots, L)$, $\mathbf{res}^{(0)} = \mathbf{Y}$, $k = 0$, $\Gamma^{(0)} = \varnothing$.

while $\left\|\mathbf{res}^{(k)}\right\|_2 > \varepsilon$

$\mathbf{v} = \left\|\boldsymbol{\Phi}'\mathbf{res}^{(k)}\right\|_{row-\infty}$. $C = \mathrm{Arg\,max}(\mathbf{v}, p)$ (i.e., select indices corresponding to p largest elements in $\mathbf{v}$)

$$k = k + 1. \quad \Gamma^{(k)} = \Gamma^{(k-1)} \cup C, \quad \mathbf{res}^{(k)} = \mathbf{Y} - \boldsymbol{\Phi}_{\Gamma^{(k)}}\boldsymbol{\Phi}^+_{\Gamma^{(k)}}\mathbf{Y}.$$

end

$\hat{\mathbf{x}}_j(\Gamma^{(k)}) = \boldsymbol{\Phi}^+_{\Gamma^{(k)}}\mathbf{y}_j, \quad \hat{\mathbf{x}}_j(\{1, 2, \ldots, N\} - \Gamma^{(k)}) = \mathbf{0}$.

In each iteration of DCS-GOMP, correlation between columns of $\boldsymbol{\Phi}$ and residual are calculated and indices of the columns corresponding to p maximal correlation are found

as the new entries of the estimated support set $\Gamma^{(k)}$. New residual is established based on $\Gamma^{(k)}$. Iterations stop only when the condition $\left\|\mathbf{res}^{(k)}\right\|_2 \leq \varepsilon$ holds true. Here ε is a very small value; typically, it can be taken as 10^{-5}. Finally, the estimates of nonzero entries of the sparse signals $\mathbf{x}_j$ $(j = 1, 2, \ldots, L)$ are obtained by LS solution $\hat{\mathbf{x}}_j(\Gamma^{(k)}) = \mathbf{\Phi}^{+}_{\Gamma^{(k)}}\mathbf{y}_j$.

3.2. **Recovery condition analysis of DCS-GOMP based on restricted isometry property (RIP).** In this section, the recovery conditions of DCS-GOMP are explored based on RIP. Some useful lemmas are listed below.

Lemma 3.1. (Lemma 3 in [12]) *If the sensing matrix satisfies the RIP of both orders M_1 and M_2, then $\delta_{M_1} \leq \delta_{M_2}$ for any $M_1 \leq M_2$.*

Lemma 3.2. (Proposition 3.1 in [11]) *For $I \subset \Omega$, if $\delta_{|I|} < 1$ then for any $\mathbf{x} \in \mathbb{R}^{|I|}$,*

$$(1 - \delta_{|I|}) \left\|\mathbf{x}\right\|_2 \leq \left\|\mathbf{\Phi}_I^{'}\mathbf{\Phi}_I\mathbf{x}\right\|_2 \leq (1 + \delta_{|I|}) \left\|\mathbf{x}\right\|_2 \tag{9}$$

$$\frac{1}{1 + \delta_{|I|}} \left\|\mathbf{x}\right\|_2 \leq \left\|(\mathbf{\Phi}_I^{'}\mathbf{\Phi}_I)^{-1}\mathbf{x}\right\|_2 \leq \frac{1}{1 - \delta_{|I|}} \left\|\mathbf{x}\right\|_2 \tag{10}$$

Lemma 3.3. (Lemma 1 in [12]) *Let I_1, $I_2 \subset \Omega$ be two disjoint sets, if $\delta_{|I_1|+|I_2|} < 1$, then*

$$\left\|\mathbf{\Phi}_{I_1}^{'}\mathbf{\Phi}\mathbf{x}\right\|_2 = \left\|\mathbf{\Phi}_{I_1}^{'}\mathbf{\Phi}_{I_2}\mathbf{x}(I_2)\right\|_2 \leq \delta_{|I_1|+|I_2|} \left\|\mathbf{x}\right\|_2 \tag{11}$$

holds for any $\mathbf{x}$ supported on I_2.

For analyzing the RIP based condition of DCS-GOMP, firstly, the condition ensuring a success at the initial iteration is discussed. Success is defined for at least one correct index is found at the iteration. Then the condition ensuring the success in non-initial iteration is explored.

3.2.1. *Condition of successful recovery at the initial iteration.* The following theorem is the sufficient condition ensuring a success of DCS-GOMP at the initial iteration.

Theorem 3.1. *Let $\mathbf{x}_j$ $(j = 1, 2, \ldots, L)$ be the sparse signals with support set Q and $p \leq |Q| = q$, then the DCS-GOMP algorithm can successfully recover sparse signals $\mathbf{x}_j$ from $\mathbf{y}_j = \mathbf{\Phi}\mathbf{x}_j$ at the initial iteration if*

$$\delta_{p+q} < \frac{1}{\sqrt{q/p} + 1} \tag{12}$$

Proof: Denote $\Gamma^{(1)}$ as the set of p indices found at the initial iteration. That means $\mathbf{\Phi}_{\Gamma^{(1)}}^{'}\mathbf{y}_j$ are p largest entries in $\mathbf{\Phi}^{'}\mathbf{y}_j$, so

$$\left\|\mathbf{\Phi}_{\Gamma^{(1)}}^{'}\mathbf{y}_j\right\|_2 = \max_{|B|=p} \sqrt{\sum_{b \in B} \left|\langle \boldsymbol{\varphi}_b, \mathbf{y}_j \rangle\right|^2} \tag{13}$$

where $\boldsymbol{\varphi}_b$ represents the b-th column of $\mathbf{\Phi}$. Note that the average of q correlation power is no larger than the average of p-best correlation power, so

$$\begin{aligned} \frac{1}{\sqrt{p}} \left\|\mathbf{\Phi}_{\Gamma^{(1)}}^{'}\mathbf{y}_j\right\|_2 &= \frac{1}{\sqrt{p}} \max_{|B|=p} \sqrt{\sum_{b \in B} \left|\langle \boldsymbol{\varphi}_b, \mathbf{y}_j \rangle\right|^2} \\ &= \max_{|B|=p} \sqrt{\frac{1}{|B|} \sum_{b \in B} \left|\langle \boldsymbol{\varphi}_b, \mathbf{y}_j \rangle\right|^2} \geq \sqrt{\frac{1}{|Q|} \sum_{b \in B} \left|\langle \boldsymbol{\varphi}_b, \mathbf{y}_j \rangle\right|^2} = \frac{1}{\sqrt{q}} \left\|\mathbf{\Phi}_Q^{'}\mathbf{y}_j\right\|_2 \end{aligned} \tag{14}$$

Using Lemma 3.2 and $\mathbf{y}_j = \mathbf{\Phi}_Q \mathbf{x}_j(Q)$ we have

$$\left\| \mathbf{\Phi}'_{\Gamma^{(1)}} \mathbf{y}_j \right\|_2 \geq \sqrt{\frac{p}{q}} \left\| \mathbf{\Phi}'_Q \mathbf{\Phi}_Q \mathbf{x}_j(Q) \right\|_2 \geq \sqrt{\frac{p}{q}} (1 - \delta_q) \left\| \mathbf{x}_j \right\|_2 \tag{15}$$

On the other hand, if $\Gamma^{(1)} \cap Q = \varnothing$, from Lemma 3.3

$$\left\| \mathbf{\Phi}'_{\Gamma^{(1)}} \mathbf{y}_j \right\|_2 \geq \left\| \mathbf{\Phi}'_{\Gamma^{(1)}} \mathbf{\Phi}_Q \mathbf{x}_j(Q) \right\|_2 \leq \delta_{p+q} \left\| \mathbf{x}_j \right\|_2 \tag{16}$$

That means if

$$\delta_{p+q} \left\| \mathbf{x}_j \right\|_2 < \sqrt{\frac{p}{q}} (1 - \delta_q) \left\| \mathbf{x}_j \right\|_2 \tag{17}$$

at least one correct index is found at the iteration. From Lemma 3.1, $\delta_q \leq \delta_{p+q}$, thus Equation (17) holds when

$$\delta_{p+q} \left\| \mathbf{x}_j \right\|_2 < \sqrt{\frac{p}{q}} (1 - \delta_{p+q}) \left\| \mathbf{x}_j \right\|_2 \tag{18}$$

i.e.,

$$\delta_{p+q} < \frac{1}{\sqrt{q/p} + 1} \tag{19}$$

As discussed above, $\Gamma^{(1)}$ contains at least one entry of Q at the initial iteration of DCS-GOMP.

3.2.2. *Success condition at non-initial iteration.* The following contents reveal the success condition of DCS-GOMP at non-initial iterations. To ensure success at $(k+1)$ iteration, two bounds should be determined. The first is the upper bound τ_p of the p-th largest correlation in magnitude between $\mathbf{res}_j^{(k)}$ and columns indexed by $F = \Omega \backslash (\Gamma^{(k)} \cup Q)$, i.e., the set of remaining incorrect indices. The second is the lower bound υ_1 of the largest correlation in magnitude between $\mathbf{res}_j^{(k)}$ and columns that indices contained in $Q - \Gamma^{(k)}$, i.e., the set of remaining correct indices. Obviously, at least one correct index is found at $(k+1)$-th iteration if $\upsilon_1 \geq \tau_p$. The following lemmas demonstrate the two bounds.

Lemma 3.4. *Let* $\tau_i = \left| \left\langle \boldsymbol{\varphi}_{\theta(i)}, \mathbf{res}_j^{(k)} \right\rangle \right|$, *where* $\theta(i) = \underset{s:s \in F \backslash \{\theta(1), \theta(2), \ldots, \theta(i-1)\}}{\arg\max} \left| \left\langle \boldsymbol{\varphi}_s, \mathbf{res}_j^{(k)} \right\rangle \right|$ *so that* τ_i *are ordered in magnitude* ($\tau_1 \geq \tau_2 \geq \cdots$). *Then,* τ_p, *the p-th largest correlation between* $\mathbf{res}_j^{(k)}$ *and* $\{\boldsymbol{\varphi}_i\}_{i \in F}$ *at (k+1)-th iteration of DCS-GOMP has an upper bound of*

$$\left(\delta_{p+q-l} + \frac{\delta_{p(1+k)} \delta_{pk+q-l}}{(1 - \delta_{pk})} \right) \frac{\left\| \mathbf{x}_j(Q - \Gamma^{(k)}) \right\|_2}{\sqrt{p}} \tag{20}$$

where l *is denoted as the number of correct indices included in* $\Gamma^{(k)}$.

The proof of Lemma 3.4 is similar to that of Lemma 3.6 in [21], except that the recovered sparse signal and residual here are $\mathbf{x}_j$ and $\mathbf{res}_j^{(k)}$, respectively. Since the recovery process is not finished yet, l is smaller than q. That means, $Q - \Gamma^{(k)}$, the set containing the rest correct indices is not empty. On the other hand, suppose newly found p indices are not overlapping with previous ones, the number of indices in $\Gamma^{(k)}$ is kp. After k successful iterations, at least k correct indices are contained in $\Gamma^{(k)}$. Under this hypothesis we can obtain $l = \left| Q - \Gamma^{(k)} \right| \geq k$.

Lemma 3.5. *Let* $\upsilon_i = \left| \left\langle \boldsymbol{\varphi}_{\theta(i)}, \mathbf{res}_j^{(k)} \right\rangle \right|$,
where $\theta(i) = \underset{s:s \in (Q - \Gamma^k) \backslash \{\theta(1), \theta(2), \ldots, \theta(i-1)\}}{\arg\max} \left| \left\langle \boldsymbol{\varphi}_s, \mathbf{res}_j^{(k)} \right\rangle \right|$ *so that* υ_i *are ordered in magnitude*

($\upsilon_1 \geq \upsilon_2 \geq \cdots$). Then, υ_1, the largest correlation between $\mathbf{res}_j^{(k)}$ and $\{\boldsymbol{\varphi}_i\}_{i\in(Q-\Gamma^{(k)})}$ at (k+1)-th iteration of DCS-GOMP has a lower bound of

$$\left(1-\delta_{q-l}-\frac{\sqrt{(1+\delta_{q-l})(1+\delta_{pk})}\delta_{pk+q-l}}{1-\delta_{pk}}\right)\frac{\left\|\mathbf{x}_j(Q-\Gamma^{(k)})\right\|_2}{\sqrt{q-l}} \tag{21}$$

The proof of Lemma 3.5 is similar to that of Lemma 3.7 in [21], except that the recovered sparse signal and residual here are $\mathbf{x}_j$ and $\mathbf{res}_j^{(k)}$, respectively. Based on these two lemmas, the condition guaranteeing success at $(k+1)$-th iteration is obtained.

Theorem 3.2. *Suppose DCS-GOMP has run k iterations successfully for recovering $\mathbf{x}_j$, then DCS-GOMP succeeds at the (k+1)-th iteration if*

$$\delta_{pq} < \frac{1}{\sqrt{q}+3} \tag{22}$$

Proof: Comparing the constants k, l, p and q, there are two obvious inequalities: $1 \leq k \leq l < q$ and $1 < p \leq q$. Note that $pk < pq$, $q-l < pq$, $pk+q-l < pq$ and $p(1+k) \leq pq$. Using Lemma 3.1, we have $\delta_{pk} < \delta_{pq}$, $\delta_{q-l} < \delta_{pq}$, $\delta_{pk+q-l} < \delta_{pq}$ and $\delta_{p(1+k)} < \delta_{pq}$.

As mentioned, the condition ensuring at least one correct index is found at the $(k+1)$ iteration is $\upsilon_1 \geq \tau_p$. From Lemma 3.4 and Lemma 3.5,

$$\begin{aligned}\tau_p &\leq \left(\delta_{p+q-l}+\frac{\delta_{p(1+k)}\delta_{pk+q-l}}{(1-\delta_{pk})}\right)\frac{\left\|\mathbf{x}_j(Q-\Gamma^{(k)})\right\|_2}{\sqrt{p}} \\ &\leq \left(\delta_{pq}+\frac{\delta_{pq}^2}{(1-\delta_{pq})}\right)\frac{\left\|\mathbf{x}_j(Q-\Gamma^{(k)})\right\|_2}{\sqrt{p}} = \frac{\delta_{pq}}{(1-\delta_{pq})}\frac{\left\|\mathbf{x}_j(Q-\Gamma^{(k)})\right\|_2}{\sqrt{p}}\end{aligned} \tag{23}$$

$$\begin{aligned}\upsilon_1 &\geq \left(1-\delta_{q-l}-\frac{\sqrt{(1+\delta_{q-l})(1+\delta_{pk})}\delta_{pk+q-l}}{1-\delta_{pk}}\right)\frac{\left\|\mathbf{x}_j(Q-\Gamma^{(k)})\right\|_2}{\sqrt{q-l}} \\ &\geq \left(1-\delta_{pq}-\frac{\sqrt{(1+\delta_{pq})(1+\delta_{pq})}\delta_{pq}}{1-\delta_{pq}}\right)\frac{\left\|\mathbf{x}_j(Q-\Gamma^{(k)})\right\|_2}{\sqrt{q-l}} \\ &= \frac{1-3\delta_{pq}}{1-\delta_{pq}}\frac{\left\|\mathbf{x}_j(Q-\Gamma^{(k)})\right\|_2}{\sqrt{q-l}}\end{aligned} \tag{24}$$

Following Equation (23) and Equation (24), the sufficient condition guaranteeing $\upsilon_1 \geq \tau_p$ is

$$\frac{1-3\delta_{pq}}{1-\delta_{pq}}\frac{\left\|\mathbf{x}_j(Q-\Gamma^{(k)})\right\|_2}{\sqrt{q-l}} > \frac{\delta_{pq}}{(1-\delta_{pq})}\frac{\left\|\mathbf{x}_j(Q-\Gamma^{(k)})\right\|_2}{\sqrt{p}} \tag{25}$$

i.e.,

$$\delta_{pq} < \frac{1}{\sqrt{(q-l)/p}+3} \tag{26}$$

Note that $q-l < pq$, Equation (26) holds true if

$$\delta_{pq} < \frac{1}{\sqrt{pq/p}+3} = \frac{1}{\sqrt{q}+3} \tag{27}$$

Thus, Theorem 3.2 is proved.

As mentioned above, the sufficient recovery conditions of DCS-GOMP at initial iteration and non-initial iteration are established, respectively.

4. **Numerical Experiments.** In this section, performance of DCS-GOMP is compared with that of DCS-SAMP, Joint-OMP and Joint-SP, in terms of the requirement for measurements, the robustness against sparsity. And also, the relationship between the number of selected indices p and successful recovery is investigated. Note that all the four algorithms can be applied in the model JSM-3; however, Joint-SP and Joint-OMP require sparsity as prior information. Algorithms proposed by [17] and [18] are only applicable to JSM-1, so they are not discussed in this section. In the end of this section, DCS-GOMP is used to recover speech signals and a sparse image, respectively. These demonstrate its application prospect.

To evaluate the performance of DCS-GOMP, L input signals whose nonzero coefficients are random Gaussian values are generated. For each signal $\mathbf{x}_j$, the common components $\mathbf{c}_j$ and independent innovation components $\mathbf{z}_j$ are assumed to be sparse with sparsity K_z and K_j, respectively. For convenience, K_j is assumed to be equal for all the signals and the measurement matrix $\mathbf{\Phi}$ is taken as an $M \times N$ random Gaussian matrix.

4.1. Comparisons among DCS-GOMP, DCS-SAMP, Joint-OMP and Joint-SP.

4.1.1. *Requirement for measurements for the four algorithms.* This experiment investigates the probability of success recovery vs. the number of measurements. DCS-SAMP, Joint-OMP, Joint-SP and DCS-GOMP are used respectively to recover signals with $N = 200$, $K_z = 15$, $K_j = 6$ and $L = 5$. The number of measurements M is a changed parameter increased from 55 to 100. 100 trials are performed to test the stability of the four algorithms against measurements. The probability of success is represented by the frequency of success. In a trial, "success" is defined for each $prec(j)$ $(j = 1, 2, \ldots, L)$ is more than 10^5, where $prec(j)$ is defined as follows:

$$prec(j) = \frac{\|\mathbf{x}_j\|_2}{\|\mathbf{x}_j - \widehat{\mathbf{x}}_j\|_2} \quad (j = 1, 2, \ldots, L) \tag{28}$$

Obviously, the larger $prec(j)$ are, the better the performance of DCS-GOMP is. The experiment result is shown in Figure 1.

The four curves with red circle, green asterisk, blue triangle and black plus represent the probability curves of success for DCS-GOMP, Joint-SP, DCS-SAMP and Joint-OMP, respectively. From Figure 1, for all the four algorithms, the probability of success increased with the increase of M. The probability curve of Joint-OMP was very close to that of Joint-SP. Performance of DCS-GOMP was better than that of Joint-OMP and Joint-SP when $M > 60$. For DCS-GOMP, the probability of success reached 0.9 when $M = 70$. Joint-SP and Joint-OMP roughly needed 75 measurements to ensure the probability of success reaching 0.9. Only requiring $M = 75$, the probability of success of DCS-GOMP reached 1. Among the four algorithms, DCS-SAMP was the worst for its high demand for M. Actually, its success probability roughly stayed at zero when M was no more than 75. To reach the probability of 0.9, DCS-SAMP required 90 measurements in this experiment. From what had been shown above, DCS-GOMP requires fewer measurements for recovery, compared with Joint-OMP, Joint-SP and DCS-SAMP.

4.1.2. *Robustness against sparsity for four algorithms.* Since DCS-GOMP is based on JSM-3, the relationship between sparsity and the performance of algorithm is explored here. In this experiment, DCS-SAMP, Joint-SP and Joint-OMP are still compared with DCS-GOMP.

Firstly, the sparsity of common components was varied in trials to investigate the performance of the four algorithms. 100 trials were performed with $N = 200$, $M = 90$,

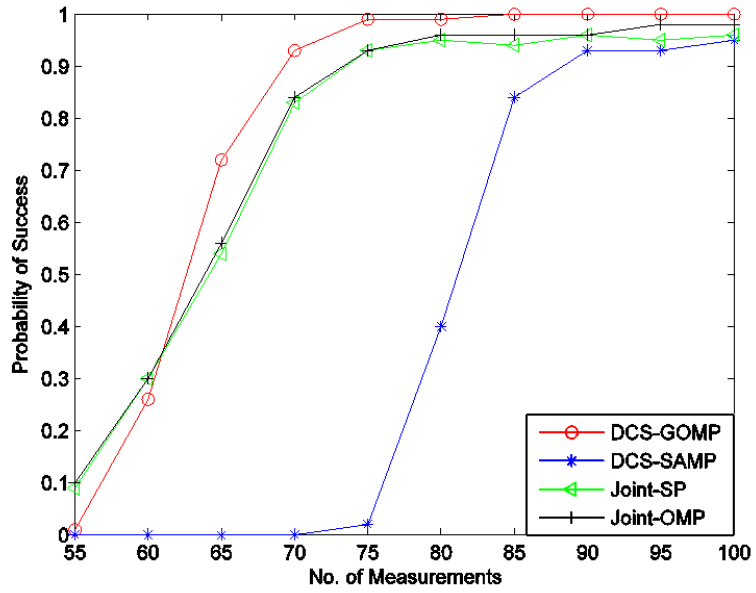

FIGURE 1. Probability of success vs. the number of measurements for DCS-SAMP, Joint-SP and Joint-OMP. The numerical values on x-axis denote the number of measurements and those on y-axis represent the probability of success for each algorithm.

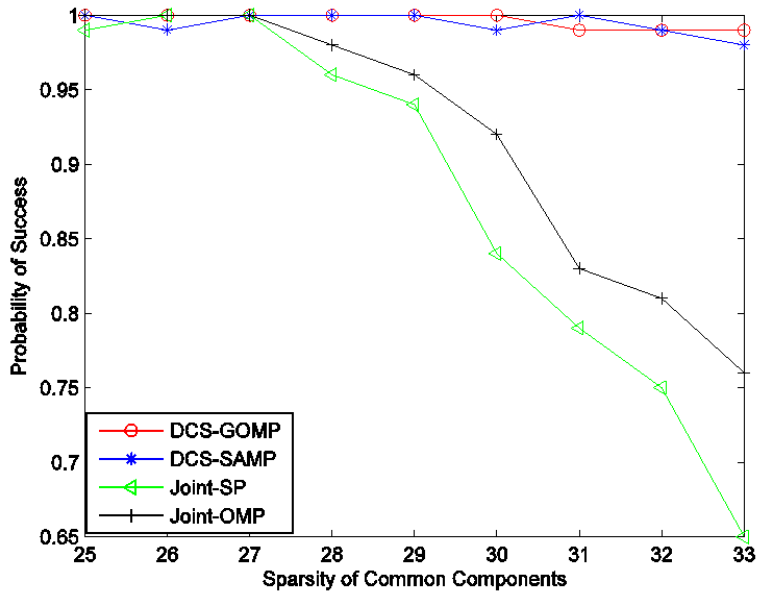

FIGURE 2. The probability of success vs. sparsity of common components for four algorithms. The numerical values on x-axis denote the sparsity of common components of signals and those on y-axis represent the probability of success for each algorithm.

$K_j = 2$ and $L = 5$. K_z was varied from 25 to 33. The result of this experiment was shown in Figure 2.

The reason why our analysis began with $K_z = 25$ lied in the fact that all of the four algorithms performed perfectly when $K_z \leq 25$. Their significant differences of performance were exposed when $K_z > 27$. When the sparsity of common components was increased from 27 to 33, the probability of success of Joint-SP and Joint-OMP both dropped rapidly. Performance of DCS-GOMP was comparable to that of DCS-SAMP. The reason why Joint-SP and Joint-OMP were sensitive to the increase of sparsity of common components might lie in the fact that the algorithms utilized the strategy of jointly finding the common support-set to recover each signal iteratively [19]. When the sparsity of common components was increased to a certain level, at which the algorithms could not successfully find the common support-set, the probability of success dropped far below 1.

Secondly, what happens when the sparsity of innovation components is increased is investigated. In this experiment, 100 trials were performed with $N = 200$, $M = 90$, $K_z = 15$ and $L = 5$. K_j was varied from 2 to 14. The experiment result was shown in Figure 3. Thanked to the fixed sparsity of common components, the probability curves for Joint-SP and Joint-OMP decreased slightly in this experiment. The probability curve of DCS-GOMP was very close to that of Joint-SP and Joint-OMP when the sparsity of innovation components was no more than 10. Once $K_j > 10$, performance of DCS-GOMP dropped rapidly. Especially, when the sparsity of innovation components was varied from 9 to 12, the success probability of DCS-GOMP dropped from 1 to 0.33. Among the four algorithms, performance of DCS-SAMP was the worst in this experiment.

4.1.3. *Performance of DCS-GOMP vs. the number of selected indices.* Since p indices are selected at each iteration of DCS-GOMP, the relationship between probability of successful recovery and the number of selected indices is investigated in this experiment.

Parameters used in this experiment were taken as $N = 200$, $M = 100$, $K_z = 15$ and $L = 5$. K_j was a changed parameter. After 100 runs, Figure 4 demonstrated probability

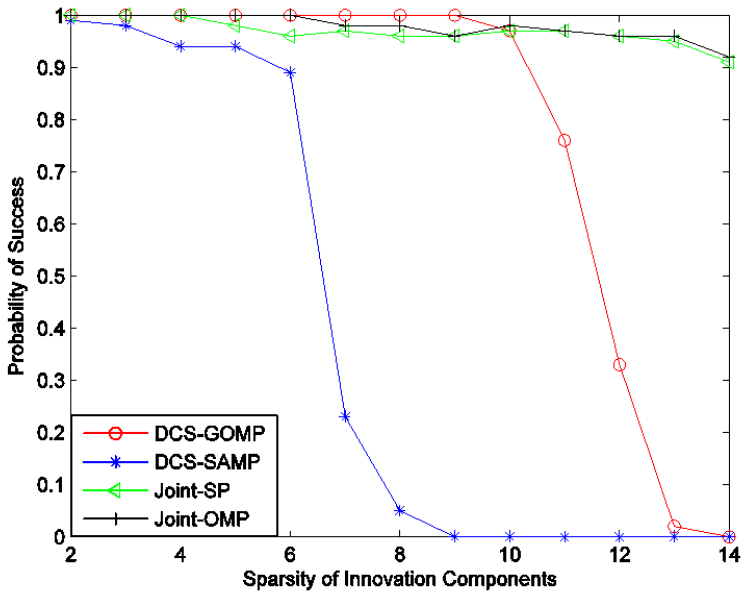

FIGURE 3. The probability of success vs. sparsity of innovation components for four algorithms. The numerical values on x-axis denote the sparsity of innovation components of signals and those on y-axis represent the probability of success for each algorithm.

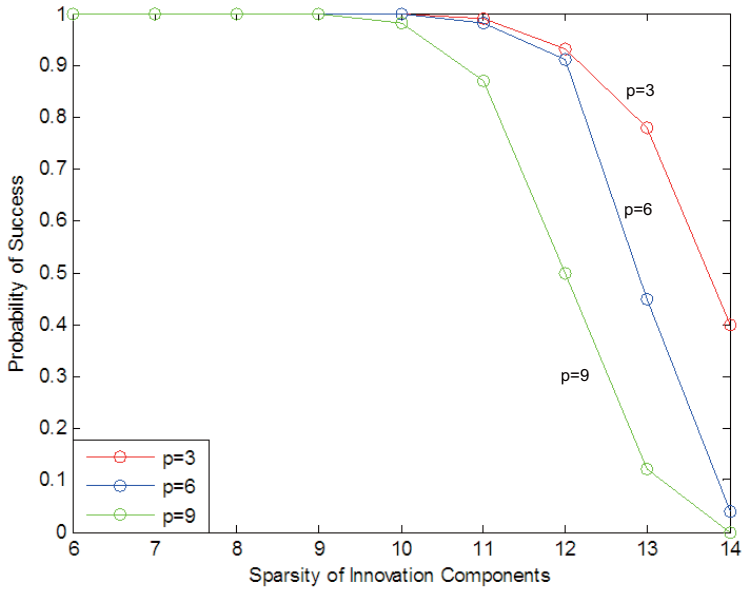

FIGURE 4. The probability of success vs. the number of selected indices p. The numerical values on x-axis denote sparsity of innovation components and those on y-axis represent the probability of success for each algorithm.

curves for $p = 3$, 6 and 9, respectively. As shown, no matter $p = 3$, 6 or 9, the probability curves dropped with the increase of K_j. However, with fixed K_j, the smaller p was, the better performance was. The significant difference among the three curves appeared when $K_j > 10$. For instance, when $K_j = 13$, the probability of success was 0.78 for $p = 3$; meanwhile, the probability of success was only 0.45 for $p = 6$. From Figure 4, the number of selected indices should be as small as possible to ensure exact recovery.

4.2. **Application of DCS-GOMP.**

4.2.1. *A DCS problem for speech signals.* In many practical scenarios, sparsity of signals are unknown. Additionally, not all signals are sparse in time domain. For practical signals that are sparse in transformed domain, DCS-GOMP can also recover them with tolerable errors.

Figure 5 presented three speech signals fragments of length $N = 1000$. Measurement matrix was a random Gaussian matrix of size 500×1000. These signals were not sparse in time domain but can be represented sparsely by discrete cosine transform (DCT). Figure 6 demonstrated their DCT coefficient vectors. Note that each DCT coefficient vector was not strictly sparse. Actually, few of its elements were significantly large while many of others were very close to zero. Viewing these coefficient vectors, one could find that their cardinalities of innovation components were not equal with each other and were much larger than cardinalities of common components. That meant the common information among these coefficient vectors was very limited. Note that joint reconstruction for DCS was based on common information among signals. These DCT coefficient vectors were measured and then reconstructed by DCS-GOMP. The recovery result was shown in Figure 7. It was obvious that all the sparse representations were recovered properly. Finally, inverse discrete cosine transform (IDCT) was applied to convert the recovered data back to time domain, and recovered the three original speech signals. The final result was demonstrated in Figure 8.

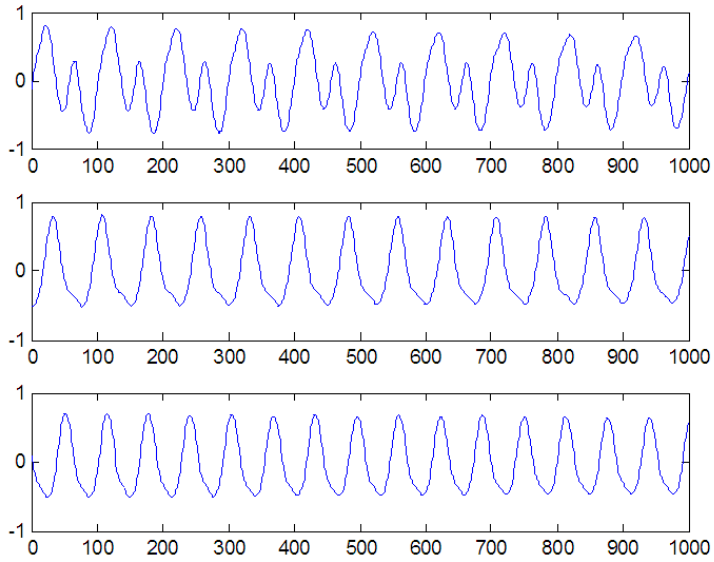

FIGURE 5. Three speech signals fragments

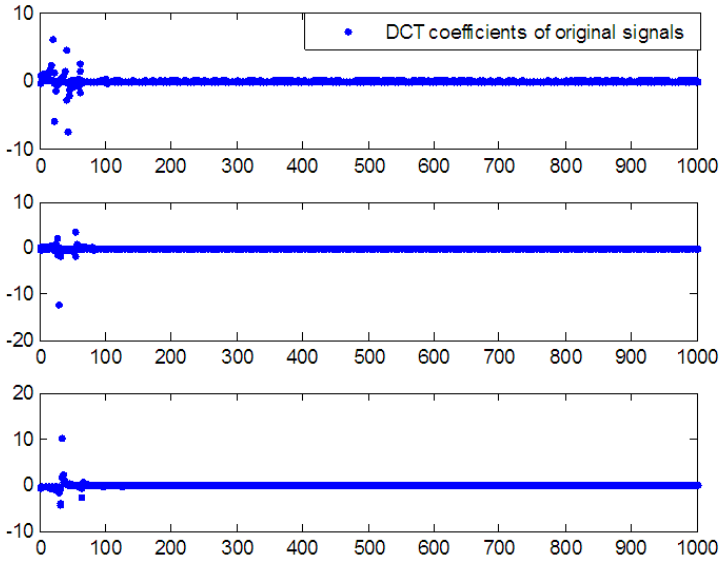

FIGURE 6. DCT coefficients of the three original signals. They were presented by blue dots.

To evaluate the recovery, 50 trials were performed. Signal-to-reconstruction-noise-ratio (SRNR) was used to evaluate the reconstruction errors, which was defined as:

$$SRNR(j) = E\left\{10\log_{10}\frac{\|\mathbf{x}_j\|_2^2}{\|\mathbf{x}_j - \hat{\mathbf{x}}_j\|_2^2}\right\}, \quad (j = 1, 2, 3) \tag{29}$$

where the calculation of mathematical expectation was replaced by an average over the number of trials. The larger SRNR was, the better the performance was. The obtained SRNR for the original signals were 29.9467, 35.8837 and 27.4723. Although the speech

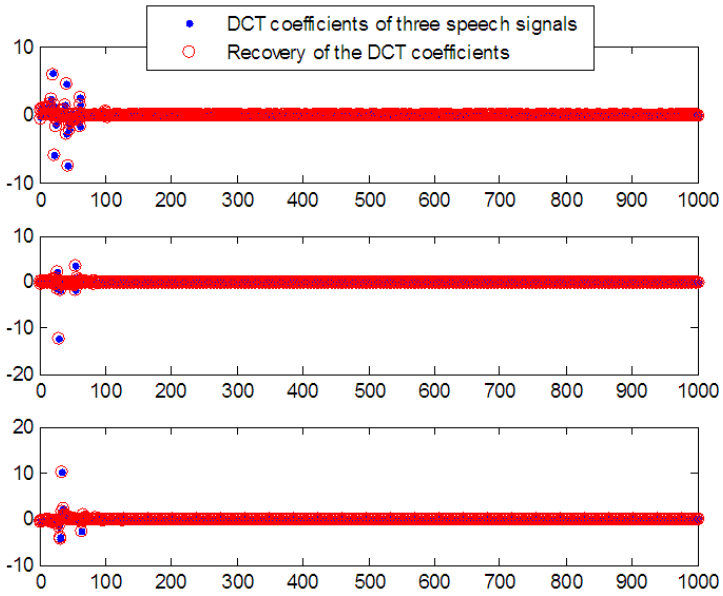

FIGURE 7. Recovery of the DCT coefficients of the original signals. Blue points represented the DCT coefficients of the original signals and red circles represented their reconstructions.

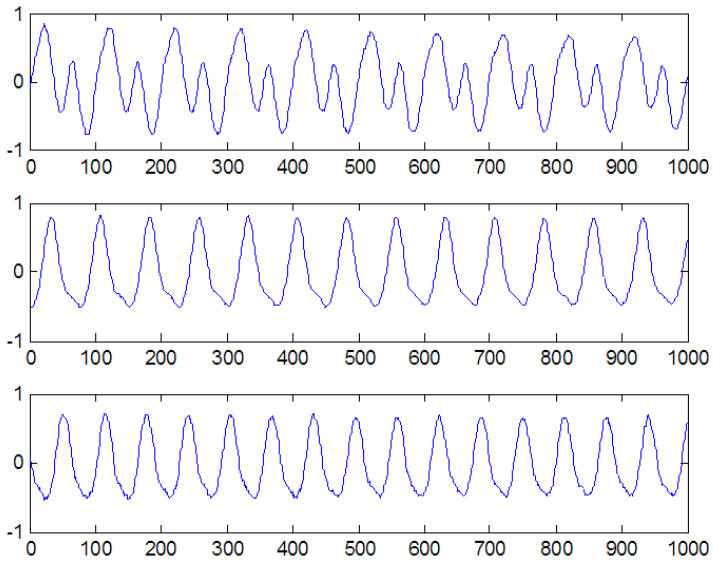

FIGURE 8. Recovery of the original speech signals

signals were not strictly sparse in transform domain and the common information was inadequate, DCS-GOMP reconstructed signals with acceptable precision. As comparisons, Joint-OMP, Joint-SP and DCS-SAMP were considered to reconstruct these speech signals. Note that both Joint-OMP and Joint-SP required sparsity as priori knowledge for reconstruction, which was not realistic for application. DCS-SAMP was a reconstructing algorithm without sparsity as priori knowledge. We used DCS-SAMP to recover these speech signals but the DCT coefficients could not be recovered correctly. Based on these

discussions, DCS-GOMP was a reliable and practical alternative for recovering speech signals, compared with existing ones.

4.2.2. *Recovery of sparse image.* In this experiment, recovery of the 256×256 image "cameraman" (Figure 9) was conducted to demonstrate the performance DCS-GOMP in realistic case. The recovery was performed using 16×16 blocks. The purpose of such processing was dividing the recovery procedure into a number of smaller, and hence simpler, procedures. Each block could be represented sparsely by 2D Haar Wavelet basis, which was dented as $\mathbf{\Psi}$. Note that for each block, wavelet coefficient vector was not strictly sparse. Actually, only few of coefficients were significantly large while many of others were very close to zero. Viewing these wavelet coefficient vectors, one can find that their cardinalities of innovation components were not equal with each other and were much larger than cardinalities of common components. Taking into account that these wavelet coefficient vectors were not sparse enough, for each block, only 30 largest magnitude wavelet coefficients were kept. For each block, the measurements were obtained via the sensing matrix $\mathbf{\Phi\Psi}$, where $\mathbf{\Phi}$ was a 128×256 measurement matrix and its entries were randomly drawn from the Gaussian distribution with mean 0 and variance 1. Denoting $\mathbf{X}_j$ and $\mathbf{Y}_j$ as the j-th block and corresponding measurements, the CS model was

$$\mathbf{Y}_j = \mathbf{\Phi\Psi X}_j = \mathbf{\Phi S}_j \tag{30}$$

where $\mathbf{S}_j = \mathbf{\Psi X}_j$ was the coefficient vector of the j-th block. Instead of recovering each coefficient vector independently, DCS-GOMP was performed to jointly recover them. In this experiment, these coefficient vectors were jointly recovered four by four. After recovering these coefficient vectors, all blocks were recovered by inverse 2D wavelet transform and then combined to obtain the whole image. Figure 10 was the recovery result that provided a Peak Signal-to-Noise Ratio (PSNR) value of 29.57. Comparing Figure 10 with Figure 9, this recovery performance was acceptable. Though these wavelet coefficient vectors are not sparse enough and cardinalities of innovation components of these wavelet coefficient vectors were not equal with each other, DCS-GOMP had recovered the image without sparsity as priori knowledge.

FIGURE 9. Test image "cameraman"

FIGURE 10. Recovery result of "cameraman" by DCS-GOMP (PSNR = 29.57)

As pointed out in 4.2.1, both Joint-OMP and Joint-SP required sparsity as priori knowledge for reconstruction, which was not realistic for application. As a comparison, DCS-SAMP was also used to recover the image in the same way as DCS-GOMP, but recovery completely failed.

5. **Conclusions.** In this paper, a new DCS algorithm, which is termed as DCS-GOMP, has been derived for joint signal recovery. In DCS-GOMP, multiple indices are selected at each iteration to estimate the support sets of signals. Extensive experiments confirm its validity and high performance, compared with other three existing DCS algorithms. The highlights of the algorithm are its capability of recovering several signals simultaneously without sparsity as prior information and its stability against the number of measurements and the sparsity of signals. Capability of solving DCS problems with unknown sparsity in realistic scenario exhibits its application perspectives. Further research is required to develop a computationally efficient version of the proposed algorithm in noisy environment as well as to better analytically characterize the performance of the algorithm.

Acknowledgment. This work is partially supported by Natural Science Foundation of China (61203287, 61302138, 11126274), Natural Science Foundation of Hubei Province (2013CFB414) and the Special Fund for Basic Scientific Research of Central Colleges, China University of Geosciences (CUGL130247). The authors also gratefully acknowledge the helpful comments and suggestions of the reviewers, which have improved the presentation.

REFERENCES

[1] D. L. Donoho, Compressed sensing, *IEEE Trans. Information Theory*, vol.52, no.4, pp.1289-1306, 2006.

[2] J. Liu, C. Z. Han and Y. Hu, A novel compressed sensing based method for reconstructing sparse signal using space-time data in airborne radar system, *Chinese Control Conference*, Xi'an, China, pp.4826-4831, 2013.

[3] H. Rauhut, K. Schnass and P. Vandergheynst, Compressed sensing and redundant dictionaries, *IEEE Trans. Information Theory*, vol.54, no.5, pp.2210-2219, 2008.

[4] E. J. Candes, J. Romberg and T. Tao, Stable signal recovery from incomplete and inaccurate measurements, *Communications on Pure and Applied Mathematics*, vol.59, no.8, pp.1207-1223, 2006.
[5] E. J. Candes, J. Romberg and T. Tao, Robust uncertainty principles: Exact signal reconstruction from highly incomplete frequency information, *IEEE Trans. Information Theory*, vol.52, no.2, pp.489-509, 2006.
[6] E. J. Candes and T. Tao, Decoding by linear programming, *IEEE Trans. Information Theory*, vol.51, no.12, pp.4203-4215, 2005.
[7] Y. Nesterov and A. Nemirovskii, *Interior-Point Polynomial Algorithms in Convex Programming*, Society for Industrial and Applied Mathematics, Philadelphia, 1994.
[8] J. A. Tropp and A. C. Gilbert, Signal recovery from random measurements via orthogonal matching pursuit, *IEEE Trans. Information Theory*, vol.53, no.12, pp.4655-4666, 2007.
[9] F. Hong, Q. B. Zhang and S. Wei, Image reconstruction based on improved backward optimized orthogonal matching pursuit algorithm, *Journal of South China University of Technology (Natural Science)*, vol.36, no.8, pp.23-27, 2008.
[10] D. Needell and R. Vershynin, Signal recovery from inaccurate and incomplete measurements via regularized orthogonal matching pursuit, *IEEE Journal of Selected Topics in Signal Process*, vol.4, no.2, pp.310-316, 2010.
[11] D. Needell and J. A. Tropp, CoSaMP: Iterative signal recovery from incomplete and inaccurate samples, *Applied and Computational Harmonic Analysis*, vol.26, no.3, pp.301-321, 2008.
[12] W. Dai and O. Milenkovic, Subspace pursuit for compressive sensing signal reconstruction, *IEEE Trans. Information Theory*, vol.55, no.5, pp.2230-2249, 2009.
[13] T. T. Do, G. Lu, N. Nguyen and T. D. Tran, Sparsity adaptive matching pursuit algorithm for practical compressed sensing, *The 42nd Asilomar Conference on Signals, Systems and Computers*, Pacific Grove, United States, pp.581-587, 2008.
[14] D. Baron, M. F. Duarte and M. B. Wakin, Distributed compressed sensing, *IEEE Trans. Information Theory*, http://dsp.rice.edu/publications/distributed-compressive-sensing, 2009.
[15] M. F. Duarte, S. Sarvotham and M. B. Wakin, Joint sparsity models for distributed compressed sensing, *Online Proc. of the Workshop on Signal Processing with Adaptive Sparse Structured Representations*, Rennes, France, 2005.
[16] D. Baron, M. F. Duarte and S. Sarvotham, An information-theoretic approach to distributed compressed sensing, *The 43rd Allerton Conference on Communication, Control, and Computing*, Monticello, United States, 2005.
[17] M. F. Duarte, S. Sarvotham and D. Baron, Distributed compressed sensing of jointly sparse signals, *The 39th Asilomar Conference on Signals, Systems and Somputers*, Pacific Grove, United States, pp.1537-1541, 2005.
[18] J. Blanchard, M. Cermak and D. Hanle, Greedy algorithms for joint sparse recovery, *IEEE Trans. Signal Processing*, vol.62, no.7, pp.1694-1704, 2014.
[19] D. Sundman, S. Chatterjee and M. Skoglund, Greedy pursuits for compressed sensing of jointly sparse signals, *European Signal Processing Conference*, Barcelona, Spain, pp.368-372, 2011.
[20] Q. Wang and Z. W. Liu, A robust and efficient algorithm for distributed compressed sensing, *Computers and Electrical Engineering*, vol.37, no.6, pp.916-926, 2011.
[21] J. Wang and B. Shin, Generalized orthogonal matching pursuit, *IEEE Trans. Signal Processing*, vol.60, no.12, pp.6202-6216, 2012.
[22] E. J. Candes, The restricted isometry property and its implications for compressed sensing, *Comptes Rendus Mathematique*, vol.346, nos.9-10, pp.589-592, 2008.